

# Modulation of gramicidin channel conformation and organization by hydrophobic mismatch in saturated phosphatidylcholine bilayers

Devaki A. Kelkar, Amitabha Chattopadhyay \*

Centre for Cellular and Molecular Biology, Uppal Road, Hyderabad 500 007, India

Received 4 August 2006; received in revised form 18 January 2007; accepted 22 January 2007

Available online 28 January 2007

## Abstract

The matching of hydrophobic lengths of integral membrane proteins and the surrounding lipid bilayer is an important factor that influences both structure and function of integral membrane proteins. The ion channel gramicidin is known to be uniquely sensitive to membrane properties such as bilayer thickness and membrane mechanical properties. The functionally important carboxy terminal tryptophan residues of gramicidin display conformation-dependent fluorescence which can be used to monitor gramicidin conformations in membranes [S.S. Rawat, D.A. Kelkar, A. Chattopadhyay, Monitoring gramicidin conformations in membranes: a fluorescence approach, *Biophys. J.* 87 (2004) 831–843]. We have examined the effect of hydrophobic mismatch on the conformation and organization of gramicidin in saturated phosphatidylcholine bilayers of varying thickness utilizing the intrinsic conformation-dependent tryptophan fluorescence. Our results utilizing steady state and time-resolved fluorescence spectroscopic approaches, in combination with circular dichroism spectroscopy, show that gramicidin remains predominantly in the channel conformation and gramicidin tryptophans are at the membrane interfacial region over a range of mismatch conditions. Interestingly, gramicidin conformation shifts toward non-channel conformations in extremely thick gel phase membranes although it is not excluded from the membrane. In addition, experiments utilizing self quenching of tryptophan fluorescence indicate peptide aggregation in thicker gel phase membranes.

© 2007 Elsevier B.V. All rights reserved.

**Keywords:** Gramicidin; Hydrophobic mismatch; REES; Acrylamide quenching

## 1. Introduction

Biological membranes are dynamic, complex entities and the structure and function of intrinsic membrane proteins are intimately linked to the membrane environment. The hydrophobic thickness of the membrane is a fundamental property of the membrane and has been found to have a profound effect on transmembrane proteins [1,2]. Hydrophobic mismatch, a difference in the hydrophobic lengths of transmembrane proteins

and the surrounding lipid annulus, can lead to changes in membrane protein folding, conformation, and activity [3–5]. Hydrophobic mismatch becomes particularly relevant in the case of ion channels, such as those formed by the linear peptide gramicidin, where channel gating is a direct consequence of conformational changes within the membrane bilayer [6]. Channel function can therefore be related to membrane deformation which is dependent on the extent of mismatch [7].

The linear pentadecapeptide gramicidin forms prototypical ion channels specific for monovalent cations and has been extensively used to study the organization, dynamics and function of membrane-spanning channels [8–10]. The gramicidin channel is formed by the transmembrane head-to-head association of single-stranded  $\beta^{6.3}$  helices [6]. In this conformation, the carboxy terminus is exposed to the membrane–water interface and the amino terminus is buried in the hydrophobic core of the membrane. This places the four carboxy terminus tryptophan residues clustered at the membrane–water interface at the entrance to the channel [6,11–13]. This membrane

**Abbreviations:** DAPC, 1,2-diarachidoyl-*sn*-glycero-3-phosphocholine [diC20:0 PC]; DCPC, 1,2-Dicapryl-*sn*-glycero-3-phosphocholine [diC10:0 PC]; DLPC, 1,2-dilauroyl-*sn*-glycero-3-phosphocholine [diC12:0 PC]; DMPC, 1,2-dimyristoyl-*sn*-glycero-3-phosphocholine [diC14:0 PC]; DPPC, 1,2-dipalmitoyl-*sn*-glycero-3-phosphocholine [diC16:0 PC]; DSPC, 1,2-distearoyl-*sn*-glycero-3-phosphocholine [diC18:0 PC]; MLV, multilamellar vesicle; REES, red edge excitation shift; SUV, small unilamellar vesicle

\* Corresponding author. Tel.: +91 40 2719 2578; fax: +91 40 2716 0311.

E-mail address: [amit@cceb.res.in](mailto:amit@cceb.res.in) (A. Chattopadhyay).

interfacial localization of tryptophan residues is a functionally important aspect of the channel conformation of gramicidin [14] and is a common feature of many transmembrane helices [15,16]. The tryptophan rich aromatic belt at the membrane interface in transmembrane helices is thought to stabilize the helix with respect to the membrane environment [15]. The experimentally determined interfacial hydrophobicity of tryptophan is the highest among the naturally occurring amino acid residues thus accounting for its specific interfacial localization in membrane-bound peptides and proteins [17]. We have earlier utilized the intrinsic tryptophan fluorescence of gramicidin to effectively distinguish gramicidin conformations in membranes [13].

The unique sequence of alternating L- and D-chirality renders gramicidin sensitive to the environment in which it is placed [18] and it adopts a wide range of environment-dependent conformations [19]. In membranes, the initial conformation of gramicidin is influenced by the nature of the solvent in which it was dissolved prior to incorporation i.e., gramicidin conformation in membranes depends on its 'solvent history' [20]. However, the channel conformation in which tryptophan residues are localized at the membrane interface, is the preferred (thermodynamically stable) conformation of gramicidin in membranes [21]. Double helical 'non-channel' conformations of gramicidin incorporated using suitable solvents [20] are thermodynamically unstable in membranes and spontaneously convert to the channel conformation [13,20,21]. The distribution and depths of the tryptophan residues constitute the major differences between these two forms [13]. In the 'non-channel' form, some of the tryptophan residues are buried in the low dielectric nonpolar region of the membrane which is an energetically unfavorable location for tryptophan residues [17]. However, the gramicidin analogue in which all the four tryptophan residues are replaced by phenylalanines, which are more hydrophobic and cannot act as hydrogen bond donors, appears to preferentially adopt the alternate antiparallel double stranded helical dimer conformation [22,23], and exhibits drastically reduced channel activity [24]. In the absence of any tryptophan residues, the non-channel conformation [double stranded helical dimer] becomes the energetically favored state in the membrane.

In situations of hydrophobic mismatch, when the energetic cost of membrane deformation is high [25], transmembrane proteins may respond by adopting an otherwise unfavorable conformation, such as the gramicidin non-channel conformation, or form lateral aggregates that would reduce the membrane exposed surface. In this work, we have employed a combination of red edge excitation shift (REES) and other fluorescence approaches, and CD spectroscopy, to monitor the effect of hydrophobic mismatch on the conformation and organization of gramicidin in membrane bilayers formed by a series of saturated phosphatidylcholines (see Table 1). In particular, we have taken advantage of the conformation-dependent fluorescence of gramicidin tryptophans to monitor conformational changes in gramicidin due to hydrophobic mismatch [13]. A shift in the wavelength of maximum

Table 1

Estimates of the hydrophobic thickness of phospholipid bilayers used

Lipid	Phase	Chain length	Hydrophobic thickness <sup>a</sup> (Å)
DCPC	Fluid	10	17.1 <sup>b</sup>
DLPC	Fluid	12	21.1 <sup>b</sup>
DMPC	Gel	14	34.0 <sup>d</sup>
DPPC	Gel	16	39.4 <sup>c</sup>
DSPC	Gel	18	44.6 <sup>c</sup>
DAPC	Gel	20	49.9 <sup>c</sup>

<sup>a</sup> The hydrophobic thickness of a bilayer is taken to be the distance between the *sn*-2 carbonyl carbons of opposing leaflet lipids [37].

<sup>b</sup> From Lewis and Engelman [37] corrected for systematic truncation errors [38]. The hydrophobic thickness has been obtained by subtracting 10.4 Å from the experimentally determined phosphate-to-phosphate transbilayer distance [39].

<sup>c</sup> Calculated using  $d_f=1.75 (n_c-1)$  and  $d_g=1.50 df$  where  $d_f$  are the hydrophobic thicknesses in the gel and fluid phase, respectively, and  $n_c$  is the number of carbon atoms in the acyl chain [40].

fluorescence emission toward higher wavelengths, caused by a shift in the excitation wavelength toward the red edge of the absorption band, is termed red edge excitation shift (REES) [26–28]. This effect is mostly observed with polar fluorophores in motionally restricted environments such as viscous solutions or condensed phases where the dipolar relaxation time for the solvent shell around a fluorophore is comparable to or longer than its fluorescence lifetime. The unique feature of REES is that while other fluorescence techniques yield information about the fluorophore itself, REES provides information about the relative rates of solvent relaxation which is not possible to obtain by other techniques. We have previously shown that REES can serve as a powerful tool to monitor gramicidin conformations in membranes and membrane-mimetic environments [12,13,29,30].

## 2. Materials and methods

### 2.1. Materials

Gramicidin A' (from *Bacillus brevis*), and 1,2-dimyristoyl-*sn*-glycero-3-phosphocholine (DMPC; diC14:0 PC) were purchased from Sigma Chemical Co. (St. Louis, MO). 1,2-Dicapryl-*sn*-glycero-3-phosphocholine (DCPC; diC10:0 PC), 1,2-dilauroyl-*sn*-glycero-3-phosphocholine (DLPC; diC12:0 PC), 1,2-dipalmitoyl-*sn*-glycero-3-phosphocholine (DPPC; diC16:0 PC), 1,2-distearoyl-*sn*-glycero-3-phosphocholine (DSPC; diC18:0 PC), and 1,2-diarachidoyl-*sn*-glycero-3-phosphocholine (DAPC; diC20:0 PC) were obtained from Avanti Polar Lipids (Alabaster, AL). Ultra pure grade acrylamide was from Gibco BRL (Rockville, MD). Gramicidin A' as obtained is a mixture of gramicidins A, B, and C. The concentration of gramicidin was calculated from its molar extinction coefficient ( $\epsilon$ ) of  $20\,700\text{ M}^{-1}\text{ cm}^{-1}$  at 280 nm [21]. The purity of acrylamide was checked from its absorbance using its molar extinction coefficient ( $\epsilon$ ) of  $0.23\text{ M}^{-1}\text{ cm}^{-1}$  at 295 nm and optical transparency beyond 310 nm [31]. Lipids were checked for purity by TLC on silica gel precoated plates (Sigma) in chloroform/methanol/water (65:35:5, v/v/v) and were found to give only one spot in all cases with a phosphate-sensitive spray and on subsequent charring [32]. The concentration of lipids was determined by phosphate assay subsequent to total digestion by perchloric acid [33]. DMPC was used as an internal standard to assess lipid digestion. All other chemicals used were of the highest purity available. Solvents used were of spectroscopic grade. Water was purified through a Millipore (Bedford, MA) Milli-Q system and used throughout.

## 2.2. Methods

### 2.2.1. Sample preparation

All experiments were done using small unilamellar vesicles (SUVs) containing 2% [mol/mol] gramicidin (except when specifically mentioned). In general, 1280 nmol of lipid in methanol/chloroform was mixed with 25.6 nmol of gramicidin in methanol. The sample was mixed well and dried under a stream of nitrogen while warming gently. After further drying under a high vacuum for at least 3 h, 1.5 ml of 10 mM sodium phosphate, 150 mM sodium chloride buffer, pH 7.2, was added and the lipid samples were hydrated (swelled) above the phase transition temperature of the lipid used [34] while being intermittently vortexed for 3 min to disperse the lipid and form homogenous multilamellar vesicles (MLVs). The MLVs so obtained were sonicated to clarity above the phase transition temperature using a Branson model 250 sonifier (Branson Ultrasonics, Dansbury, CT) fitted with a microtip. The sonicated samples were then centrifuged at 15000 rpm for 15 min at room temperature to remove titanium particles shed from the microtip during sonication. Samples were incubated for at least 8 h at 65 °C (or ~15 °C above the phase transition temperature of the lipid used) to induce the channel conformation [13,20]. Background samples were prepared in the same way except that gramicidin was omitted. Samples in the gel phase were incubated in dark for at least 8 h below the phase transition temperature before any measurements were made. All experiments were done at 25 °C except in experiments involving DMPC where temperature was set at 17 °C.

### 2.2.2. Steady state fluorescence measurements

Steady state fluorescence measurements were performed with a Hitachi F-4010 spectrofluorometer (Tokyo, Japan) using 1 cm path length quartz cuvettes. Excitation and emission slits with a nominal bandpass of 5 nm were used for all measurements. Background intensities of samples in which gramicidin was omitted were subtracted from each sample spectrum to cancel out any contribution due to the solvent Raman peak and other scattering artifacts. The spectral shifts obtained with different sets of samples were identical in most cases, or were within  $\pm 1$  nm of the ones reported. In samples where gramicidin to lipid ratios were varied, gramicidin and lipid concentration were kept low to avoid any artifacts in measurements of fluorescence intensity due to scattering or inner filter effects (Fig. 6). In addition, fluorescence intensity values were normalized to a specific gramicidin/lipid ratio to account for variations in fluorescence intensity due to instrumental conditions. Fluorescence polarization measurements were performed using a Hitachi polarization accessory. Polarization values were calculated from the equation [35]:

$$P = \frac{I_{VV} - GI_{VH}}{I_{VV} + GI_{VH}} \quad (1)$$

where  $I_{VV}$  and  $I_{VH}$  are the measured fluorescence intensities (after appropriate background subtraction) with the excitation polarizer vertically oriented and emission polarizer vertically and horizontally oriented, respectively.  $G$  is the grating correction factor and is the ratio of the efficiencies of the detection system for vertically and horizontally polarized light, and is equal to  $I_{HV}/I_{HH}$ . All experiments were done with multiple sets of samples and average values of polarization are shown in Table 2.

### 2.2.3. Acrylamide quenching

Acrylamide quenching experiments of gramicidin tryptophan fluorescence were carried out by measurement of fluorescence intensity in separate samples containing increasing amounts of acrylamide taken from a freshly prepared 4 M stock solution in water. Samples were kept in dark for at least 1 h before measuring fluorescence. The excitation wavelength used was 295 nm and emission was monitored at 334 nm. Corrections for inner filter effect were made using the following equation [35]:

$$F = F_{\text{obs}} \text{antilog}[(A_{\text{ex}} + A_{\text{em}})/2] \quad (2)$$

where  $F$  is the corrected fluorescence intensity and  $F_{\text{obs}}$  is the background subtracted fluorescence intensity of the sample.  $A_{\text{ex}}$  and  $A_{\text{em}}$  are the measured absorbances at the excitation and emission wavelengths. The absorbances of the samples were measured using a Hitachi U-2000 UV-visible absorption spectro-

Table 2

Fluorescence emission characteristics of gramicidin in membranes of different hydrophobic thickness

Lipid	Phase	Fluorescence emission maximum (nm) <sup>a</sup>	Fluorescence polarization <sup>b</sup>
DCPC	Fluid	334	0.110±0.002
DLPC	Fluid	332	0.113±0.001
DMPC	Gel	332	0.099±0.002
DPPC	Gel	333	0.103±0.002
DSPC	Gel	335	0.126±0.003
DAPC	Gel	338	0.074±0.003

<sup>a</sup> Lipid concentration was 0.85 mM and the ratio of gramicidin to lipid was 1:50 (mol/mol) in all cases. All other conditions are as in Fig. 1. The excitation wavelength was 280 nm. See Materials and methods for other details.

<sup>b</sup> Calculated using Eq. (1). The polarization value represents mean±SE of at least three independent measurements. The ratio of gramicidin/lipid was 1:50 (mol/mol) and the concentration of gramicidin was 4.4 μM. The excitation wavelength was 280 nm and the emission was set at 330 nm. All other conditions are as in Fig. 1. See Materials and methods for other details.

photometer. Quenching data were analyzed by fitting to the Stern–Volmer equation [35]:

$$F_0/F = 1 + K_{SV}[Q] = 1 + k_q\tau_0[Q] \quad (3)$$

where  $F_0$  and  $F$  are the fluorescence intensities in the absence and presence of the quencher, respectively,  $[Q]$  is the molar quencher concentration and  $K_{SV}$  is the Stern–Volmer quenching constant. The Stern–Volmer quenching constant  $K_{SV}$  is equal to  $k_q\tau_0$  where  $k_q$  is the bimolecular quenching constant and  $\tau_0$  is the intensity-averaged lifetime of the fluorophore in the absence of quencher.

### 2.2.4. Time-resolved fluorescence measurements

Fluorescence lifetimes were calculated from time-resolved fluorescence intensity decays using a Photon Technology International (London, Western Ontario, Canada) LS-100 luminescence spectrophotometer in the time-correlated single photon counting mode. This machine uses a thyatron-gated nanosecond flash lamp filled with nitrogen as the plasma gas (17±1 in. of mercury vacuum) and is run at 17–20 kHz. Lamp profiles were measured at the excitation wavelength using Ludox (colloidal silica) as the scatterer. To optimize the signal to noise ratio, 5000 photon counts were collected in the peak channel. The excitation wavelength used was 297 nm and emission was set at 330 nm. All experiments were performed using excitation and emission slits with a bandpass of 10 nm or less. The sample and the scatterer were alternated after every 10% acquisition to ensure compensation for shape and timing drifts occurring during the period of data collection. This arrangement also prevents any prolonged exposure of the sample to the excitation beam thereby avoiding any possible photodamage to the fluorophore. The data stored in a multichannel analyzer was routinely transferred to an IBM PC for analysis. Fluorescence intensity decay curves so obtained were deconvoluted with the instrument response function and analyzed as a sum of exponential terms:

$$F(t) = \sum_i \alpha_i \exp(-t/\tau_i) \quad (4)$$

where  $F(t)$  is the fluorescence intensity at time  $t$  and  $\alpha_i$  is a pre-exponential factor representing the fractional contribution to the time-resolved decay of the component with a lifetime  $\tau_i$  such that  $\sum_i \alpha_i = 1$ . The decay parameters were recovered using a nonlinear least squares iterative fitting procedure based on the Marquardt algorithm as described previously [13]. A fit was considered acceptable when plots of the weighted residuals and the autocorrelation function showed random deviation about zero with a minimum  $\chi^2$  value generally not more than 1.5. Intensity-averaged lifetimes  $\langle \tau \rangle$  for biexponential decays of fluorescence were calculated from the decay times and pre-exponential factors using the following equation [35]:

$$\langle \tau \rangle = \frac{\alpha_1 \tau_1^2 + \alpha_2 \tau_2^2}{\alpha_1 \tau_1 + \alpha_2 \tau_2} \quad (5)$$

### 2.2.5. Circular dichroism measurements

CD measurements were carried out at room temperature (25 °C; for DMPC the temperature was set at 17 °C) on a JASCO J-715 spectropolarimeter (Tokyo, Japan) which was calibrated with [+]-10-camphorsulfonic acid. The spectra were scanned in a quartz optical cell with a path length of 0.1 cm. All spectra were recorded in 0.5 nm wavelength increments with a 4 sec response and a band width of 1 nm. For monitoring changes in secondary structure, spectra were scanned from 200 to 280 nm at a scan rate of 100 nm/min. Each spectrum is the average of 12 scans with a full scale sensitivity of 10 mdeg. All spectra were corrected for background by subtraction of appropriate blanks and were smoothed making sure that the overall shape of the spectrum remains unaltered. Data are represented as mean residue ellipticities and were calculated using the formula:

$$[\theta] = \theta_{\text{obs}} / (10Cl) \quad (6)$$

where  $\theta_{\text{obs}}$  is the observed ellipticity in mdeg,  $l$  is the path length in cm, and  $C$  is the concentration of peptide bonds in mol/L.

### 2.2.6. Sucrose density gradient centrifugation

Continuous sucrose gradients (0–8%) were prepared with a total volume of 9 ml of 10 mM sodium phosphate, 150 mM sodium chloride buffer, pH 7.2. SUVs were prepared as described earlier using 2560 nmol DAPC and 51.2 nmol gramicidin, and 1.5 ml of the sample was carefully layered on the top of the gradient. The samples were then centrifuged for 20 h at  $150\,000 \times g$  at 25 °C in a Beckmann SW-41 rotor (Beckmann Instruments, Palo Alto, CA). After centrifugation, fractions of 500  $\mu$ l were manually collected from the top of the gradient and the relative peptide and lipid contents were estimated. Relative peptide content was estimated by measuring fluorescence at 334 nm when excited at 280 nm. Relative lipid content was determined from the 90° light scattering intensity at 450 nm using a Hitachi F-4010 spectrofluorometer. The fraction densities and sucrose concentration were determined by measurement of refractive index using a Schmidt and Haensch refractometer.

## 3. Results

In general, the extent of mismatch between the hydrophobic thickness of the membrane and the protein determines the mismatch response [36]. Table 1 shows estimates for the hydrophobic thickness of the various bilayers used in this study. We have used a series of saturated lipids in the gel phase (except for DCPC and DLPC) to form bilayers of increasing thickness. We chose to use saturated lipids of different acyl chain lengths since lipid unsaturation is known to influence the conformational preference of gramicidin [41,42]. In addition, gel phase membranes are known to be less compressible than the corresponding fluid phase [43]. Reduced compressibility would imply that the energetic cost of membrane deformation required for hydrophobic matching would be higher [25], which could possibly promote protein conformational change as a mismatch adaptation. While the gramicidin dimer is  $\sim 26$  Å thick [9], the functional hydrophobic thickness of gramicidin is generally considered to be  $\sim 22$  Å [44]. Interestingly, the length of the double helical dimer (non-channel form) has been reported to be 31 Å [9]. Since the estimates for the hydrophobic lengths of the bilayers used vary between  $\sim 17.1$  and 49.9 Å (see Table 1), incorporation of gramicidin in these bilayers would result in hydrophobic mismatch.

### 3.1. Gramicidin conformation in membranes of varying thickness as monitored by circular dichroism

Circular dichroism spectroscopy has been previously used to characterize gramicidin conformations [9,13,20]. To

ensure the formation of the gramicidin channel conformation as the initial conformation, sonicated samples were incubated overnight at high temperature [13,20] followed by incubation below the phase transition temperature of the lipid used to allow the samples to reach an equilibrium conformation (see Materials and methods for details of sample preparation). The CD spectra of gramicidin in membranes of varying hydrophobic thickness prepared this way are shown in Fig. 1. A typical CD spectrum of the gramicidin channel conformation has two characteristic peaks of positive ellipticity at  $\sim 218$  and 235 nm, a valley at  $\sim 230$  nm, and negative ellipticity below 208 nm. Double helical non-channel conformations, on the other hand, are characterized by a large negative peak at 229 nm, a weaker positive peak at 218 nm, and positive ellipticity below 208 nm [13,20,21]. As can be seen from Fig. 1, the CD spectra in thinner membranes (up to DPPC) are typical of the channel conformation. Interestingly, there is a reduction in peak intensity with increasing chain length. However, in thicker membranes (DSPC and DAPC), both peaks are of weaker intensity, and the spectra tend toward the spectrum of the double helical non-channel conformation [13]. The reduction in the intensity of peaks characteristic of the channel conformation could indicate a transition toward non-channel conformations. However lateral aggregation [see later] within the membrane has also been reported to reduce CD spectral intensity [45]. A significant reduction in the typical CD spectrum of the channel conformation with increasing chain length has been previously reported [46]. A possible reason for the more significant reduction in these early results compared to the present results could be that the ‘solvent history’ property of gramicidin conformation [20,21] was not accounted for in the earlier work. This may be important since the rate of conversion from the non-channel to channel form has been found to be chain length dependent [21].

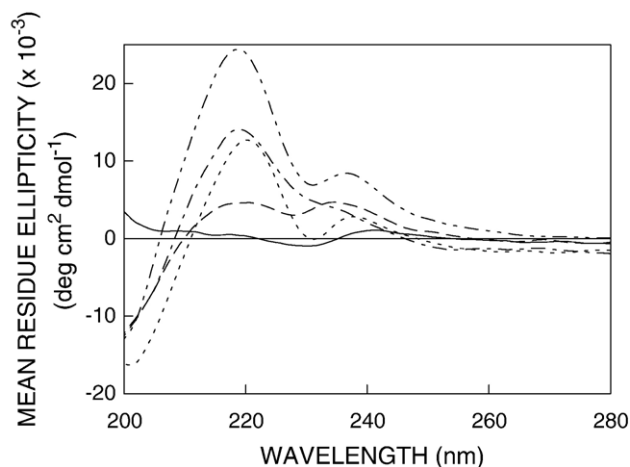


Fig. 1. Far-UV CD spectra of gramicidin in DLPC (· · · ·), DMPC (---), DPPC (- · - ·), DSPC (— — —), and DAPC (—) membranes. Lipid concentration was 0.85 mM and the ratio of gramicidin to lipid was 1:50 (mol/mol) in all cases. All experiments were done at 25 °C except for DMPC where temperature was maintained at 17 °C. See Materials and methods for other details.

### 3.2. Fluorescence characteristics and lifetimes of gramicidin in membranes of varying thickness

Table 2 shows the fluorescence characteristics of gramicidin in membranes of varying hydrophobic thickness. The fluorescence emission maximum of gramicidin is found to be dependent on the chain length of the lipid used and varies from 332 nm in DMPC to 338 nm in DAPC bilayers. Interestingly, the emission maximum displays a red shift in very thick or very thin bilayers. This could indicate that there is increased water penetration around the gramicidin tryptophans in very thick bilayers or even in thinner bilayers [see acrylamide quenching experiments later] as a result of increased bilayer deformation and/or changes in gramicidin conformation [13]. Such bilayer thickness-dependent emission maxima have earlier been observed for a reporter tryptophan in a model transmembrane peptide placed in the middle of the bilayer [47]. However, tryptophan residues that act as membrane interface anchors generally do not show mismatch-dependent emission maxima [48,49]. Therefore, observation of mismatch-dependent emission maxima for gramicidin could be indicative of specific conformational changes in response to hydrophobic mismatch.

The steady state fluorescence polarization values for gramicidin tryptophans in membranes of varying thickness are shown in Table 2. In general, the fluorescence polarization values are indicative of tryptophans located at the motionally restricted membrane interface [12,13]. Importantly, the polarization in DAPC is reduced as compared to the corresponding values for other lipids. Such reduced polarization values for gramicidin tryptophans in membranes have earlier been shown to be characteristic of the ‘non-channel’ conformation of gramicidin [13].

Fluorescence lifetime serves as a sensitive indicator for the local environment and polarity in which a given fluorophore is placed [50]. A typical decay profile of gramicidin tryptophans in DSPC membranes with its biexponential fitting and the various statistical parameters used to check the goodness of the fit are shown in Fig. 2. The fluorescence lifetimes of gramicidin tryptophans in membranes of varying thickness are shown in Table 3. As seen from the table, all fluorescence decays could be fitted well with a biexponential function. We chose to use the mean fluorescence lifetime as an important parameter for describing the behavior of gramicidin tryptophans in membranes of varying thickness since it is independent of the number of exponentials used to fit the time-resolved fluorescence decay. The intensity-averaged fluorescence lifetimes of gramicidin tryptophans in membranes of varying thickness calculated using Eq. (5) are shown in Table 3. In general, the mean fluorescence lifetimes obtained for gramicidin in membranes of varying thickness ( $\leq 2$  ns) are indicative of the channel conformation [13]. Interestingly, in DAPC bilayers, the mean fluorescence lifetime of gramicidin is significantly increased ( $\sim 2.6$  ns). Such increased lifetimes have earlier been reported for gramicidin in the non-channel conformation [13]. An increase in polarity of the tryptophan environment is known to reduce the lifetime of tryptophans due to fast deactivating processes in polar environments

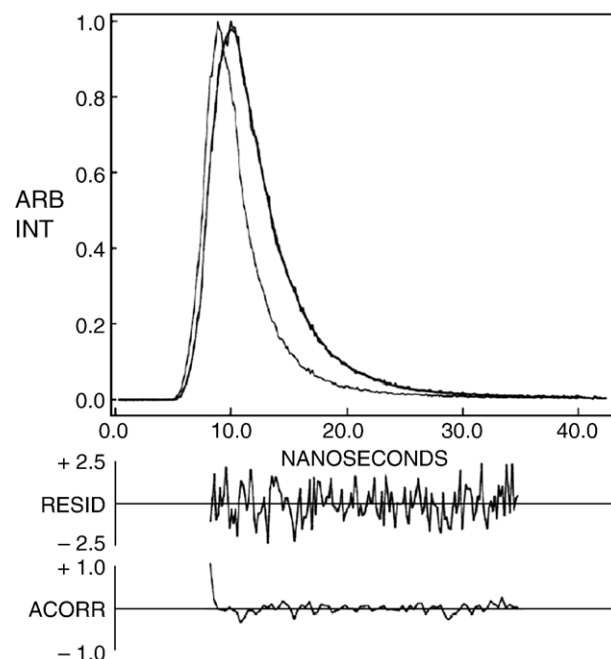


Fig. 2. Representative time-resolved fluorescence intensity decay of gramicidin in DSPC vesicles. Excitation was at 297 nm which corresponds to a peak in the spectral output of the nitrogen lamp. Emission was monitored at 330 nm. The sharp peak on the left is the lamp profile. The relatively broad peak on the right is the decay profile, fitted to a biexponential function. The two lower plots show the weighted residuals and the autocorrelation function of the weighted residuals. Concentration of lipid was 0.85 mM and the ratio of gramicidin to lipid was 1:50 (mol/mol). See Materials and methods for other details.

[51,52]. The increase in mean fluorescence lifetime of the tryptophans in the non-channel conformation could therefore be attributed to the localization of some of the tryptophan residues in the deeper hydrophobic region of the membrane in this conformation.

### 3.3. Red edge excitation shift of gramicidin in membranes of different hydrophobic thickness

Red edge excitation shift (REES) represents a powerful approach which can be used to directly monitor the environment and dynamics around a fluorophore in a complex biological system [27,28]. Importantly, we have previously shown that REES of gramicidin tryptophans can be effectively used to distinguish gramicidin conformations in membranes [13]. The shifts in the maxima of fluorescence emission<sup>1</sup> of the tryptophan residues of gramicidin in DLPC and DAPC membranes as a function of excitation wavelength are shown in Fig. 3a (for other membranes, see 3b). A more comprehensive representation of the magnitude of REES obtained for

<sup>1</sup> We have used the term maximum of fluorescence emission in a somewhat wider sense here. In every case, we have monitored the wavelength corresponding to maximum fluorescence intensity, as well as the center of mass of the fluorescence emission. In most cases, both these methods yielded the same wavelength. In cases where minor discrepancies were found, the center of mass of emission has been reported as the fluorescence maximum.

Table 3  
Intensity-averaged fluorescence lifetimes of gramicidin tryptophans in membranes of different hydrophobic thickness<sup>a</sup>

Lipid	$\alpha_1$	$\tau_1$ (ns)	$\alpha_2$	$\tau_2$ (ns)	$\langle\tau\rangle^b$ (ns)
DCPC	0.16	3.63	0.84	1.14	2.08
DLPC	0.15	3.22	0.85	0.80	1.81
DMPC	0.19	3.41	0.81	0.95	2.07
DPPC	0.11	3.64	0.89	0.68	1.86
DSPC	0.08	3.88	0.92	0.68	1.74
DAPC	0.12	4.74	0.88	0.68	2.66

<sup>a</sup> The excitation wavelength was 297 nm; emission was monitored at 340 nm. All other conditions are as in Fig. 1. See Materials and methods for other details.

<sup>b</sup> Calculated using Eq. (5).

gramicidin in membranes of varying hydrophobic thickness is shown in Fig. 3b. In very thin fluid phase bilayers (DCPC and DLPC), as the excitation wavelength is changed from 280 to 310 nm, the emission maximum is shifted from 334 to 340 nm in DCPC and 332 to 338 nm in DLPC bilayers. This corresponds to a REES of 6 nm in both cases. It is possible that there could be further red shift if excitation is carried out beyond 310 nm. We found it difficult to work in this wavelength range due to low signal to noise ratio and artifacts due to the solvent Raman peak that sometimes remained even after background subtraction. Such dependence of the emission maximum on excitation wavelength is characteristic of the red edge excitation shift. This implies that the gramicidin tryptophans in these membranes, on the average, are localized in a motionally restricted region of the membrane. This is consistent with the membrane interfacial localization of the gramicidin tryptophans in the channel conformation [11–13].

Fig. 3 also shows the magnitude of REES for gramicidin tryptophans in thicker membranes in the gel phase. Surprisingly, gramicidin tryptophans do not display any REES in thick bilayers, while in relatively thin bilayers (DMPC) gramicidin tryptophans display a reduced REES of 2 nm (see Fig. 3b). We have recently shown that reduced REES of gramicidin tryptophan is characteristic of non-channel conformations where some of the tryptophan residues are buried in the deeper regions of the membrane bilayer [13]. This region of the membrane is more isotropic (bulk hydrocarbon-like) and is characterized by lower polarity. Importantly, the deeper hydrophobic region of the membrane is more dynamic as compared to the interfacial region [53,54], and is characterized by less pronounced red edge effects [27,54,55]. In addition, fluorophores embedded in gel phase membranes in general, show reduced REES as compared to the corresponding fluid phase [54, Kelkar, D. A. and A. Chattopadhyay, unpublished observations]. A combination of these factors could be responsible for the absence of any measurable REES in thicker (DPPC–DAPC) membranes.

#### 3.4. Acrylamide quenching of gramicidin fluorescence in membranes of varying thickness

Acrylamide quenching of tryptophan fluorescence is widely used to monitor tryptophan environments in proteins [56]. Fig. 4 shows representative Stern–Volmer plots of acrylamide quench-

ing of gramicidin tryptophans in bilayers of various thickness (Stern–Volmer plots for only selected bilayers are shown for clarity). The slope ( $K_{SV}$ ) of such a plot is related to the accessibility (degree of exposure) of the tryptophans to the quencher. The quenching parameter obtained by analyzing the Stern–Volmer plot is shown in Table 4. The Stern–Volmer constant ( $K_{SV}$ ) for acrylamide quenching appears to be dependent to some extent on the hydrophobic thickness of the membrane (0.53 to 0.95  $M^{-1}$ ). Interestingly, in DAPC membranes the accessibility of tryptophan residues to acrylamide is increased and the  $K_{SV}$  is found to be 1.77  $M^{-1}$ . The increased accessibility of gramicidin tryptophan residues in DAPC bilayers corresponds well with the reported value for the non-channel conformation in membranes [13]. However,

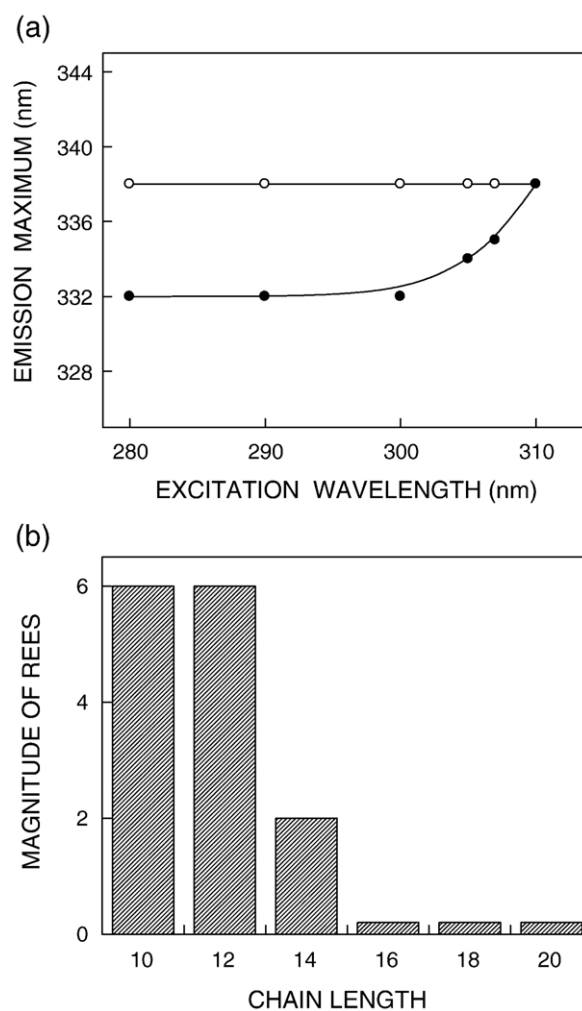


Fig. 3. (a) Effect of changing excitation wavelength on the wavelength of maximum emission for gramicidin in DLPC (●), and DAPC (○) membranes (similar data for gramicidin in other membranes are not shown for clarity). (b) A comprehensive representation of the magnitude of REES obtained for gramicidin tryptophans in membranes of varying thickness. The magnitude of REES corresponds to the total shift in emission maximum when the excitation wavelength is changed from 280 to 310 nm (as in (a)). Note the reduced REES in gel phase membranes regardless of chain length. No REES was observed in DPPC, DSPC, and DAPC membranes (the bars are shown only for clarity). All conditions are as in Fig. 1. See Materials and methods for other details.

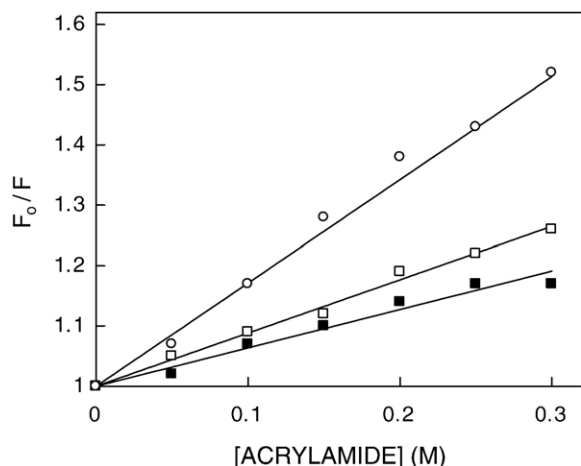


Fig. 4. Representative data for Stern-Volmer analysis of acrylamide quenching of gramicidin fluorescence in gel phase DMPC (■), DSPC (□), and DAPC (○) membranes.  $F_0$  is the fluorescence in the absence of quencher, and  $F$  is the fluorescence in the presence of quencher. Concentration of lipid was 0.11 mM and the ratio of gramicidin to lipid was 1:50 (mol/mol). All other conditions are as in Fig. 1. The excitation wavelength was fixed at 295 nm and emission was monitored at 334 nm in all cases. See Materials and methods for other details.

interpretation of the Stern–Volmer constant is complicated this way due to its intrinsic dependence on fluorescence lifetime (see Eq. (3)). The bimolecular quenching constant ( $k_q$ ) for acrylamide quenching is therefore a more accurate measure of the degree of exposure since  $k_q$  takes into account differences in fluorescence lifetime. The bimolecular quenching constants, calculated using Eq. (3), are shown in Table 4. The  $k_q$  values show that the relative accessibility of gramicidin tryptophans is dependent on membrane hydrophobic thickness although the differences are small. The lowest value is obtained for DMPC which corresponds well with the relatively blue shifted fluorescence emission maxima of gramicidin in DMPC membranes (see Table 2).

### 3.5. Exclusion of gramicidin from thick mismatched membranes

A possible consequence of hydrophobic mismatch, besides bilayer thickening/thinning and protein conformational change within the membrane, is the exclusion of the protein from the membrane phase [57,58]. Such a mismatch adaptation is especially relevant for gel phase membranes that have reduced compressibility, since the energetic cost of bilayer deformation would be high [25]. In addition, surface orientations for lysine flanked mismatched peptides have been reported [47]. This can be ruled out as a possibility for gramicidin due to the high hydrophobicity of the gramicidin sequence [9]. We performed sucrose density centrifugation of gramicidin containing DAPC vesicles to check for any excluded (from the bulk membrane phase) peptide-rich aggregate. Fig. 5 shows the sucrose density pattern obtained of the distribution of lipid (DAPC) and gramicidin in a linear gradient of sucrose. The gradient exhibits coincident peaks of both lipid and gramicidin, indicating that gramicidin is associated with the lipid. This rules out the possibility that gramicidin is excluded from DAPC bilayers. However, this does not exclude the possibility that gramicidin may form lateral aggregates within the membrane.

Table 4

Acrylamide quenching of gramicidin fluorescence in membranes of different hydrophobic thickness<sup>a</sup>

Lipid	Phase	$K_{SV}^b$ ( $M^{-1}$ )	$k_q$ ( $\times 10^{-9}$ ) <sup>c</sup> ( $M^{-1} s^{-1}$ )
DCPC	Fluid	$0.95 \pm 0.04$	0.46
DLPC	Fluid	$0.87 \pm 0.07$	0.48
DMPC	Gel	$0.53 \pm 0.02$	0.26
DPPC	Gel	$0.81 \pm 0.06$	0.44
DSPC	Gel	$0.77 \pm 0.02$	0.44
DAPC	Gel	$1.77 \pm 0.06$	0.67

<sup>a</sup> Concentration of lipid was 0.11 mM and the ratio of gramicidin to lipid was 1:50 (mol/mol). The excitation wavelength was 295 nm; emission was monitored at 334 nm. All other conditions are as in Fig. 1. See Materials and methods for other details.

<sup>b</sup> Calculated using Eq. (3). The quenching parameter shown represents the mean  $\pm$  SE of multiple independent measurements while quenching data shown in Fig. 3 are from representative experiments.

<sup>c</sup> Calculated using intensity-averaged fluorescence lifetimes from Table 3 and using Eq. (3).

### 3.6. Lateral aggregation in thick membranes monitored using tryptophan self quenching

Lateral aggregation is a possible mismatch adaptation that can be employed by membrane proteins and peptides to reduce the extent of unfavorable interactions with the membrane [2]. Aggregation within the membrane would be dependent on the lateral concentration (i.e., peptide to lipid molar ratio) of the peptide within the membrane. Self quenching of fluorescence upon lateral aggregation [59–62] can be used as a convenient tool to monitor lateral aggregation in membranes [61]. Tryptophan fluorescence has previously been found to be susceptible to self quenching upon aggregation (Chattopadhyay, A. and R. Rukmini, unpublished observations).

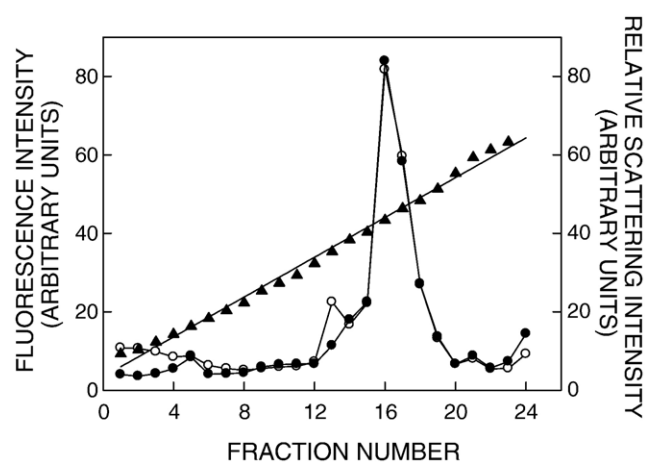


Fig. 5. Sucrose density gradient analysis of DAPC vesicles containing gramicidin. The ratio of gramicidin to lipid was 1:50 (mol/mol). Percent sucrose (▲) was determined by the refractive index and ranged from 0.93–6.3% at the end points. Relative amount of gramicidin (●) in each fraction was determined by measuring the fluorescence intensity at 334 nm when excited at 280 nm. The relative amount of lipid in each fraction (○) was determined from the 90° light scattering intensity at 450 nm. See Materials and methods for other details.

We utilized the lateral concentration-dependent self quenching of gramicidin tryptophans to monitor possible mismatch-dependent aggregation. We used a series of samples with increasing gramicidin lateral concentration (i.e., mol% gramicidin). In the absence of any lateral aggregation within the membrane, there should be a linear increase in fluorescence intensity with increasing gramicidin concentration, as observed for a methanolic solution of gramicidin in the same concentration range (data not shown). In situations where lateral aggregation occurs, the increase in fluorescence intensity will deviate from linearity. Importantly, if self quenching is indeed indicative of aggregation, the gramicidin mol% at which the deviation from linearity occurs, must show chain length dependence.

In DPPC membranes (see Fig 6a), fluorescence intensity increases linearly with lateral concentration. However at very high mol percent (~4 mol%) of gramicidin, the plot appears to slightly deviate from linearity indicating possible aggregation at this gramicidin to lipid ratio (see Fig. 6a). In DSPC and DAPC membranes (Fig. 6b and c), deviation from linearity occurs at even lower mol% (~2.5 and 1.5 mol%, respec-

tively). Thus, the threshold gramicidin to lipid ratio at which self quenching of fluorescence intensity is observed is inversely related to the thickness of the membrane (see Fig. 6d). As predicted, aggregation begins at lower lateral concentrations in thicker membranes. Our assumption that self quenching is indicative of aggregation is therefore valid. An important caveat of these results is that we have only monitored those aggregates where gramicidin tryptophan residues are in close proximity leading to fluorescence self quenching. Interestingly, earlier studies using atomic force microscopy in supported gel phase bilayers have reported the formation of hexameric aggregates of gramicidin at a similar range of concentrations in DPPC bilayers [63].

#### 4. Discussion

Gramicidin serves as an excellent model for transmembrane channels due to its small size, ready availability and the relative ease with which chemical modifications can be performed. This makes gramicidin unique among small membrane-active peptides and provides the basis for the use of gramicidin to

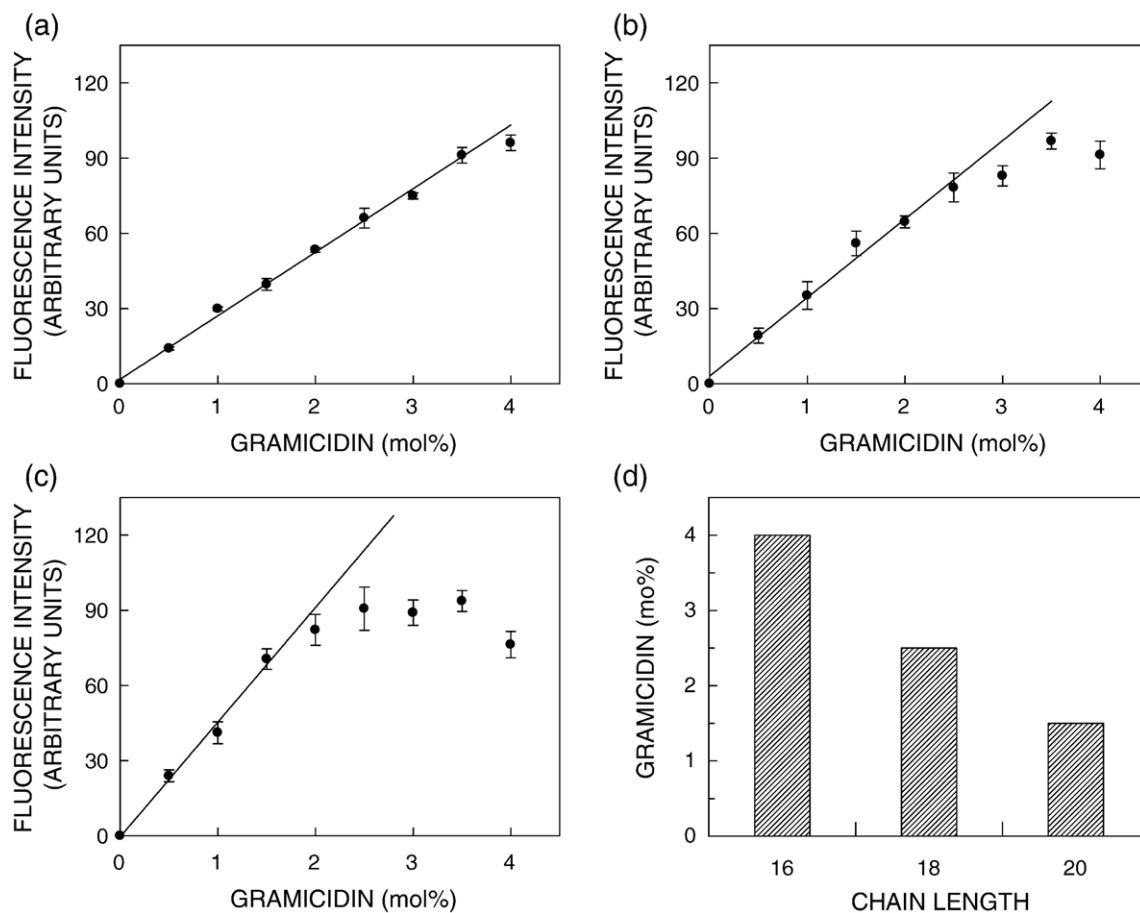


Fig. 6. Change in fluorescence intensity of gramicidin as a function of increasing gramicidin to lipid ratio in vesicles of (a) DPPC (b) DSPC and (c) DAPC. Fluorescence intensity was measured at 334 nm when excited at 280 nm. The lipid concentration was 200  $\mu$ M for DSPC and DPPC, and 100  $\mu$ M in the case of DAPC at all gramicidin to lipid ratios. The concentration of gramicidin was between 0.5 to 8  $\mu$ M. Each sample was prepared separately. Fluorescence intensity values are normalized to a specific gramicidin/lipid ratio. The data represent the mean  $\pm$  SE of multiple independent measurements. See Materials and methods for other details. The mol% gramicidin at which the increase in fluorescence intensity deviates from linearity is shown in (d) as a function of chain length.

explore the principles that govern the folding and function of membrane-spanning channels in particular, and membrane proteins in general. Importantly, the possibility of alternate, membrane-bound conformations of gramicidin provides a unique opportunity to study the effects of the membrane environment on protein conformation (and function) in a simple model system.

In this work, we have utilized the conformation-dependent fluorescence of the gramicidin tryptophans to monitor conformational changes in gramicidin due to hydrophobic mismatch. We show that gramicidin conformation tends to shift toward otherwise thermodynamically unfavorable, non-channel conformations in very thick bilayers. Interestingly, it was previously shown that gramicidin channel function is directly related to membrane thickness [44,64,65]. The reduction in functional channels upon increase in membrane thickness has been explained as an increase in the proportion of double stranded gramicidin dimers (i.e., non-channel conformations) [64]. A transition from the channel toward non-channel conformations has earlier been shown to occur in saturated DPPC and DSPC bilayers [66,67]. In thin fluid phase bilayers, mismatch adaptation occurs by the overall change in thickness of the membrane bilayer [68], specifically by the ordering of the lipid annular layers [69] as predicted by the ‘Mattress Model’ [36], rather than by a change in helical pitch [70]. Therefore, in thin membranes, the tryptophan residues would be located at the membrane interface, while in thicker membranes, tryptophan residues would be located across the membrane bilayer as in the non-channel conformation [13].

This supplements previous results, using CD and NMR spectroscopy and high performance size exclusion chromatography, where it was shown that non-channel conformations predominate in very thin chain lipid environments, and a membrane bilayer of  $\geq 10$  acyl chain length is required for the channel conformation [71]. Interestingly, it has recently been shown that the extent of mismatch adaptation is related to the nature of the membrane exposed surface of the mismatched protein [72]. Thus, while gramicidin tends to significantly alter the thickness of mismatched bilayers, single helical tryptophan flanked peptides have a reduced effect on lipid thickness. This implies that packing of lipid chains around a single helix is fundamentally different from the way lipid chains pack against a larger protein surface such as gramicidin [72]. This could also explain why gramicidin is not excluded from the membrane phase even under extreme mismatch conditions in gel phase membranes, while transmembrane  $\alpha$ -helical peptides are excluded from thick bilayers [57,58]. We also show that gramicidin tends to form concentration-dependent aggregates in thick mismatched bilayers. We have utilized the concentration-dependent quenching of tryptophan fluorescence to assess aggregation in these systems.

A well-documented response of gramicidin to mismatch associated with high lateral concentrations of gramicidin is phase change from the lamellar to inverted hexagonal ( $H_{II}$ ) phase [73–75]. It has been clearly demonstrated that the propensity of gramicidin to induce the  $H_{II}$  phase is chain length dependent, occurring at lower lateral concentrations in

membranes with longer acyl chain length [76–78]. The possibility of the formation of  $H_{II}$  at the high concentrations used in Fig. 6 could therefore be a matter of concern. Interestingly, gramicidin induced formation of the  $H_{II}$  phase is primarily associated with membranes in the fluid phase [79]. However, gramicidin is known to affect lipid phase behavior [80]. A systematic study of the gramicidin induced  $H_{II}$  phase in DPPC and DSPC fluid phase bilayers showed that  $H_{II}$  phase formation in these membranes starts at 13 mol% and 6 mol%, respectively [78]. Based on these previous results, we can eliminate the possibility of the formation of  $H_{II}$  phases in DPPC and DSPC at the highest concentration used (4 mol%) in Fig. 6. In addition, the macroscopic phase separation associated with  $H_{II}$  phase formation [81] is not observed for gramicidin containing DAPC membranes at 2 mol% (see Fig. 5).

It is important to emphasize that the conformational change in membrane-bound gramicidin from the non-functional non-channel conformations to the functional channel conformation [13,82] is a consequence of the preference of tryptophan residues to reside at the membrane interface [17]. Thus, while gramicidin is a unique peptide in sequence and structure, its membrane-bound conformation is influenced by lipid–protein interactions that are universal [83]. In this paper, we have monitored gramicidin tryptophan environments in a series of saturated membrane systems taking advantage of the conformation-dependent fluorescence of gramicidin [13]. We show that under conditions of extreme mismatch, the gramicidin channel conformation converts to the otherwise unfavorable non-channel conformation.

## Acknowledgements

This work was supported by the Council of Scientific and Industrial Research, Government of India. D.A.K. would like to thank the Council of Scientific and Industrial Research for the award of a Senior Research Fellowship. A.C. is an Honorary Professor of the Jawaharlal Nehru Centre for Advanced Scientific Research, Bangalore (India). We are grateful to Dr. K.G. Harikumar for his help with the sucrose density gradient experiments and Satinder Rawat for useful discussions in the early part of this work. We thank Y.S.S.V. Prasad and G.G. Kingi for technical help and members of our laboratory for critically reading the manuscript.

## References

- [1] M.Ø. Jensen, O.G. Mouritsen, Lipids do influence protein function—The hydrophobic mismatch hypothesis revisited, *Biochim. Biophys. Acta* 1666 (2004) 205–226.
- [2] A.G. Lee, How lipids affect the activities of integral membrane proteins, *Biochim. Biophys. Acta* 1666 (2004) 62–87.
- [3] J.H. Kleinschmidt, L.K. Tamm, Secondary and tertiary structure formation of the  $\beta$ -barrel membrane protein OmpA is synchronized and depends on membrane thickness, *J. Mol. Biol.* 324 (2002) 319–330.
- [4] I.M. Williamson, S.J. Alvis, J.M. East, A.G. Lee, Interactions of phospholipids with the potassium channel KcsA, *Biophys. J.* 83 (2002) 2026–2038.
- [5] F. Dumas, J.-F. Tocanne, G. Leblanc, M.-C. Lebrun, Consequences of

- hydrophobic mismatch between lipids and melibiose permease on melibiose transport, *Biochemistry* 39 (2000) 4846–4854.
- [6] A.M. O'Connell, R.E. Koeppe, O.S. Andersen, Kinetics of gramicidin channel formation in lipid bilayers: transmembrane monomer association, *Science* 250 (1990) 1256–1259.
- [7] O.S. Andersen, C. Nielsen, A.M. Maer, J.A. Lundbæk, M. Goulian, R.E. Koeppe, Ion channels as tools to monitor lipid bilayer–membrane protein interactions: gramicidin channels as molecular force transducers, *Methods Enzymol.* 294 (1999) 208–224.
- [8] O.S. Andersen, R.E. Koeppe, Molecular determinants of channel function, *Physiol. Rev.* 72 (1992) 89–158.
- [9] J.A. Killian, Gramicidin and gramicidin–lipid interactions, *Biochim. Biophys. Acta* 1113 (1992) 391–425.
- [10] B.A. Wallace, Common structural features in gramicidin and other ion channels, *BioEssays* 22 (2000) 227–234.
- [11] R.R. Ketchum, W. Hu, T.A. Cross, High-resolution conformation of gramicidin A in a lipid bilayer by solid-state NMR, *Science* 261 (1993) 1457–1460.
- [12] S. Mukherjee, A. Chattopadhyay, Motionally restricted tryptophan environments at the peptide–lipid interface of gramicidin channels, *Biochemistry* 33 (1994) 5089–5097.
- [13] S.S. Rawat, D.A. Kelkar, A. Chattopadhyay, Monitoring gramicidin conformations in membranes: a fluorescence approach, *Biophys. J.* 87 (2004) 831–843.
- [14] O.S. Andersen, D.V. Greathouse, L.L. Providence, M.D. Becker, R.E. Koeppe, Importance of tryptophan dipoles for protein function: 5—Fluorination of tryptophans in gramicidin A channels, *J. Am. Chem. Soc.* 120 (1998) 5142–5146.
- [15] R.A.F. Reithmeier, Characterization and modeling of membrane proteins using sequence analysis, *Curr. Opin. Struct. Biol.* 5 (1995) 491–500.
- [16] M.B. Ulmschneider, M.S.P. Sansom, Amino acid distributions in integral membrane protein structures, *Biochim. Biophys. Acta* 1512 (2001) 1–14.
- [17] W.C. Wimley, S.H. White, Experimentally determined hydrophobicity scale for proteins at membrane interfaces, *Nat. Struct. Biol.* 3 (1996) 842–848.
- [18] A. Chattopadhyay, D.A. Kelkar, Ion channels and D-amino acids, *J. Biosci.* 30 (2005) 147–149.
- [19] W.R. Veatch, E.T. Fossel, E.R. Blout, The conformation of gramicidin A, *Biochemistry* 13 (1974) 5249–5256.
- [20] P.V. LoGrasso, F. Moll, T.A. Cross, Solvent history dependence of gramicidin A conformations in hydrated lipid bilayers, *Biophys. J.* 54 (1988) 259–267.
- [21] J.A. Killian, K.U. Prasad, D. Hains, D.W. Urry, The membrane as an environment of minimal interconversion. A circular dichroism study on the solvent dependence of the conformational behavior of gramicidin in diacylphosphatidylcholine model membranes, *Biochemistry* 27 (1988) 4848–4855.
- [22] M. Cotten, F. Xu, T.A. Cross, Protein stability and conformational rearrangements in lipid bilayers: linear gramicidin, a model system, *Biophys. J.* 73 (1997) 614–623.
- [23] D. Salom, E. Pérez-Payá, J. Pascal, C. Abad, Environment- and sequence-dependent modulation of the double-stranded to single-stranded conformational transition of gramicidin A in membranes, *Biochemistry* 37 (1998) 14279–14291.
- [24] V. Fonseca, P. Daumas, L. Ranjalaly-Rasoloarijao, F. Heitz, R. Lazaro, Y. Trudelle, O.S. Andersen, Gramicidin channels that have no tryptophan residues, *Biochemistry* 31 (1992) 5340–5350.
- [25] J.A. Lundbæk, O.S. Andersen, T. Werge, C. Nielsen, Cholesterol-induced protein sorting: an analysis of energetic feasibility, *Biophys. J.* 84 (2003) 2080–2089.
- [26] A.P. Demchenko, The red-edge effects: 30 years of exploration, *Luminescence* 17 (2002) 19–42.
- [27] A. Chattopadhyay, Exploring membrane organization and dynamics by the wavelength-selective fluorescence approach, *Chem. Phys. Lipids.* 122 (2003) 3–17.
- [28] H. Raghuraman, D.A. Kelkar, A. Chattopadhyay, Novel insights into protein structure and dynamics utilizing the red edge excitation shift approach, in: C.D. Geddes, J.R. Lakowicz (Eds.), *Reviews in Fluorescence* 2005, Vol. 2, Springer, New York, 2005, pp. 199–224.
- [29] S.S. Rawat, D.A. Kelkar, A. Chattopadhyay, Effect of structural transition of the host assembly on dynamics of an ion channel peptide: a fluorescence approach, *Biophys. J.* 89 (2005) 3049–3058.
- [30] D.A. Kelkar, A. Chattopadhyay, Effect of graded hydration on the dynamics of an ion channel peptide: a fluorescence approach, *Biophys. J.* 88 (2005) 1070–1080.
- [31] M.R. Eftink, Fluorescence quenching reactions: Probing biological macromolecular structure, in: T.G. Dewey (Ed.), *Biophysical and Biochemical Aspects of Fluorescence Spectroscopy*, Plenum Press, New York, 1991, pp. 1–41.
- [32] J.C. Dittmer, R.L. Lester, A simple, specific spray for the detection of phospholipids on thin-layer chromatograms, *J. Lipid Res.* 5 (1964) 126–127.
- [33] C.W.F. McClare, An accurate and convenient organic phosphorus assay, *Anal. Biochem.* 39 (1971) 527–530.
- [34] R. Koynova, M. Caffrey, Phases and phase transitions of the phosphatidylcholines, *Biochim. Biophys. Acta* 1376 (1998) 91–145.
- [35] J.R. Lakowicz, *Principles of fluorescence spectroscopy*, Kluwer-Plenum Press, New York, 1999.
- [36] O.G. Mouritsen, M. Bloom, Mattress model of lipid–protein interactions in membranes, *Biophys. J.* 46 (1984) 141–153.
- [37] B.A. Lewis, D.M. Engelman, Lipid bilayer thickness varies linearly with acyl chain length in fluid phosphatidylcholine vesicles, *J. Mol. Biol.* 166 (1983) 211–217.
- [38] P. Balgavý, M. Dubničková, N. Kučerka, M.A. Kiselev, S.P. Yaradaikin, D. Uhríková, Bilayer thickness and lipid interface area in unilamellar extruded 1,2-diacylphosphatidylcholine liposomes: a small-angle neutron scattering study, *Biochim. Biophys. Acta* 1512 (2001) 40–52.
- [39] J.F. Nagle, S. Tristram-Nagle, Structure of lipid bilayers, *Biochim. Biophys. Acta* 1469 (2000) 159–195.
- [40] M.M. Sperotto, O.G. Mouritsen, Dependence of lipid membrane phase transition temperature on the mismatch of protein and lipid hydrophobic thickness, *Eur. Biophys. J.* 16 (1988) 1–10.
- [41] S.V. Sychev, L.I. Barsukov, V.T. Ivanov, The double  $\pi\pi 5.6$  helix of gramicidin A predominates in unsaturated lipid membranes, *Eur. Biophys. J.* 22 (1993) 279–288.
- [42] S.S. Rawat, Lipid–protein interaction: organization and dynamics of the ion channel-forming peptide gramicidin in membranes and micelles, PhD thesis, Jawaharlal Nehru University, New Delhi, India, 1998.
- [43] D. Needham, E. Evans, Structure and mechanical properties of giant lipid (DMPC) vesicle bilayers from 20 °C below to 10 °C above the liquid crystalline phase transition at 24 °C, *Biochemistry* 27 (1988) 8261–8269.
- [44] J.R. Elliott, D. Needham, J.P. Dilger, D.A. Haydon, The effects of bilayer thickness and tension on gramicidin single-channel lifetime, *Biochim. Biophys. Acta* 735 (1983) 95–103.
- [45] R.W. Woody, Circular dichroism, *Methods Enzymol.* 246 (1995) 34–71.
- [46] B.A. Wallace, W.R. Veatch, E.R. Blout, Conformation of gramicidin A in phospholipid vesicles: circular dichroism studies of effects of ion binding, chemical modification, and lipid structure, *Biochemistry* 20 (1981) 5754–5760.
- [47] J. Ren, S. Lew, Z. Wang, E. London, Transmembrane orientation of hydrophobic  $\alpha$ -helices is regulated both by the relationship of helix length to bilayer thickness and by the cholesterol concentration, *Biochemistry* 36 (1997) 10213–10220.
- [48] M.R.R. de Planque, E. Goormatigh, D.V. Greathouse, R.E. Koeppe, J.A. W. Kruijtz, R.M.J. Liskamp, B. de Kruijff, J.A. Killian, Sensitivity of single membrane-spanning  $\alpha$ -helical peptides to hydrophobic mismatch with a lipid bilayer: effects on backbone structure, orientation, and extent of membrane incorporation, *Biochemistry* 40 (2001) 5000–5010.
- [49] A.M. Powl, J.M. East, A.G. Lee, Heterogeneity in the binding of lipid molecules to the surface of a membrane protein: hot spots for anionic lipids on the mechanosensitive channel of large conductance MscL and effects on conformation, *Biochemistry* 44 (2005) 5873–5883.
- [50] F.G. Prendergast, Time-resolved fluorescence techniques: methods and applications in biology, *Curr. Opin. Struct. Biol.* 1 (1991) 1054–1059.
- [51] E.P. Kirby, R.F. Steiner, The influence of solvent and temperature upon the fluorescence of indole derivatives, *J. Phys. Chem.* 74 (1970) 4480–4490.

- [52] C. Ho, C.D. Stubbs, Hydration at the membrane protein–lipid interface, *Biophys. J.* 63 (1992) 897–902.
- [53] M. Moser, D. Marsh, P. Meier, K.-H. Wassmer, G. Kothe, Chain configuration and flexibility gradient in phospholipid membranes. Comparison between spin-label electron spin resonance and deuterium nuclear magnetic resonance, and identification of new conformations, *Biophys. J.* 55 (1989) 111–123.
- [54] A. Chattopadhyay, S. Mukherjee, Red edge excitation shift of a deeply embedded membrane probe: implications in water penetration in the bilayer, *J. Phys. Chem., B* 103 (1999) 8180–8185.
- [55] A. Chattopadhyay, S. Mukherjee, Depth-dependent solvent relaxation in membranes: wavelength-selective fluorescence as a membrane dipstick, *Langmuir* 15 (1999) 2142–2148.
- [56] M.R. Eftink, Fluorescence quenching: theory and applications, in: J.R. Lakowicz (Ed.), *Topics in fluorescence spectroscopy. Vol. 2: Principles*, Plenum Press, New York, 1991, pp. 53–126.
- [57] R.J. Webb, J.M. East, A.G. Lee, Hydrophobic mismatch and the incorporation of peptides into lipid bilayers: a possible mechanism for retention in the Golgi, *Biochemistry* 37 (1998) 673–679.
- [58] Y. Yano, M. Ogura, K. Matsuzaki, Measurement of thermodynamic parameters for hydrophobic mismatch 2: intermembrane transfer of a transmembrane helix, *Biochemistry* 45 (2006) 3379–3385.
- [59] A.L. Plant, Mechanism of concentration quenching of a xanthene dye encapsulated in phospholipid vesicles, *Photochem. Photobiol.* 44 (1986) 453–459.
- [60] R.F. Chen, J.R. Knutson, Mechanism of fluorescence concentration quenching of carboxyfluorescein in liposomes: energy transfer to nonfluorescent dimers, *Anal. Biochem.* 172 (1988) 61–77.
- [61] A. Chattopadhyay, S.S. Komath, B. Raman, Aggregation of lasalocid A in membranes: a fluorescence study, *Biochim. Biophys. Acta* 1104 (1992) 147–150.
- [62] Y. Yano, K. Matsuzaki, Measurement of thermodynamic parameters for hydrophobic mismatch 1: self-association of a transmembrane helix, *Biochemistry* 45 (2006) 3370–3378.
- [63] J. Mou, D.M. Czajkowsky, Z. Shao, Gramicidin A aggregation in supported gel phase phosphatidylcholine bilayers, *Biochemistry* 35 (1996) 3222–3226.
- [64] N. Mobashery, C. Nielsen, O.S. Andersen, The conformational preference of gramicidin channels is a function of lipid bilayer thickness, *FEBS Lett.* 412 (1997) 15–20.
- [65] B. Martinac, O.P. Hamill, Gramicidin A channels switch between stretch activation and stretch inactivation depending on bilayer thickness, *Proc. Natl. Acad. Sci. U. S. A.* 99 (2002) 4308–4312.
- [66] M. Zein, R. Winter, Effect of temperature, pressure and lipid acyl chain length on the structure and phase behaviour of phospholipid-gramicidin bilayers, *Phys. Chem. Chem. Phys.* 2 (2000) 4545–4551.
- [67] B.G. Dzikovski, P.P. Borbat, J.H. Freed, Spin-labeled gramicidin A: channel formation and dissociation, *Biophys. J.* 87 (2004) 3504–3517.
- [68] T.A. Harroun, W.T. Heller, T.M. Weiss, L. Yang, H.W. Huang, Experimental evidence for hydrophobic matching and membrane-mediated interactions in lipid bilayers containing gramicidin, *Biophys. J.* 76 (1999) 937–945.
- [69] M.R.R. de Planque, D.V. Greathouse, R.E. Koeppe, H. Schäfer, D. Marsh, J.A. Killian, Influence of lipid/peptide hydrophobic mismatch on the thickness of diacylphosphatidylcholine bilayers. A  $^2\text{H}$  NMR and ESR study using designed transmembrane  $\alpha$ -helical peptides and gramicidin A, *Biochemistry* 37 (1998) 9333–9345.
- [70] J. Katsaras, R.S. Prosser, R.H. Stinson, J.H. Davis, Constant helical pitch of the gramicidin channel in phospholipid bilayers, *Biophys. J.* 61 (1992) 827–830.
- [71] D.V. Greathouse, J.F. Hinton, K.S. Kim, R.E. Koeppe, Gramicidin A/short-chain phospholipid dispersions: chain length dependence of gramicidin conformation and lipid organization, *Biochemistry* 33 (1994) 4291–4299.
- [72] T.M. Weiss, P.C.A. van der Wel, J.A. Killian, R.E. Koeppe, H.W. Huang, Hydrophobic mismatch between helices and lipid bilayers, *Biophys. J.* 84 (2003) 379–385.
- [73] V. Chupin, J.A. Killian, B. de Kruijff,  $^2\text{H}$ -nuclear magnetic resonance investigations on phospholipid acyl chain order and dynamics in the gramicidin-induced hexagonal HII phase, *Biophys. J.* 51 (1987) 395–405.
- [74] R. Brasseur, J.A. Killian, B. de Kruijff, J.M. Ruysschaert, Conformational analysis of gramicidin–gramicidin interactions at the air/water interface suggests that gramicidin aggregates into tube-like structures similar as found in the gramicidin-induced hexagonal  $\text{H}_{\text{II}}$  phase, *Biochim. Biophys. Acta* 903 (1987) 11–17.
- [75] J.A. Killian, K.U. Prasad, D.W. Urry, B. de Kruijff, A mismatch between the length of gramicidin and the lipid acyl chains is a prerequisite for HII phase formation in phosphatidylcholine model membranes, *Biochim. Biophys. Acta* 978 (1989) 341–345.
- [76] C.J.A. van Echteld, B. de Kruijff, A.J. Verkleij, J. Leunissen-Bijvelt, J. de Gier, Gramicidin induces the formation of non-bilayer structures in phosphatidylcholine dispersions in a fatty acid chain length dependent way, *Biochim. Biophys. Acta* 692 (1982) 126–138.
- [77] B.A. Cornell, L.E. Weir, F. Separovic, The effect of gramicidin A on phospholipid bilayers, *Eur. Biophys. J.* 16 (1988) 113–119.
- [78] P.I. Watnick, S.I. Chan, P. Dea, Hydrophobic mismatch in gramicidin A/ $\gamma$ -lecithin systems, *Biochemistry* 29 (1990) 6215–6221.
- [79] J.A. Killian, B. de Kruijff, Thermodynamic, motional, and structural aspects of gramicidin-induced hexagonal HII phase formation in phosphatidylethanolamine, *Biochemistry* 24 (1985) 7881–7890.
- [80] M.R. Morrow, G.A. Simatos, R. Srinivasan, N. Grandal, L. Taylor, K.M.W. Keough, The effect of changes in gramicidin conformation on bilayer lipid properties, *Biochim. Biophys. Acta* 1070 (1991) 209–214.
- [81] J.A. Killian, K.N.J. Burger, B. de Kruijff, Phase separation and hexagonal HII phase formation by gramicidins A, B and C in dioleoylphosphatidylcholine model membranes. A study on the role of the tryptophan residues, *Biochim. Biophys. Acta* 897 (1987) 269–284.
- [82] S. Arumugam, S. Pascal, C.L. North, W. Hu, K.-C. Lee, M. Cotten, R.R. Ketchum, F. Xu, M. Brenneman, F. Kovacs, F. Tian, A. Wang, S. Huo, T.A. Cross, Conformational trapping in a membrane environment: a regulatory mechanism for protein activity? *Proc. Natl. Acad. Sci. U. S. A.* 93 (1996) 5872–5876.
- [83] D.A. Kelkar, A. Chattopadhyay, Membrane interfacial localization of aromatic amino acids and membrane protein function, *J. Biosci.* 31 (2006) 297–302.